Inorg. Chem. **2008**, *47*, 10479−10490

A Dinuclear Ni(I) System Having a Diradical Ni_2N_2 Diamond Core Resting State: Synthetic, Structural, Spectroscopic Elucidation, and Reductive Bond Splitting Reactions

Debashis Adhikari,[†] Susanne Mossin,[‡] Falguni Basuli,[§] Benjamin R. Dible,[||] Mircea Chipara,[⊥] Hongjun Fan,[†] John C. Huffman,[†] Karten Meyer,*[,‡] and Daniel J. Mindiola*[,†]

Department of Chemistry and the Molecular Structure Center, Indiana University, Bloomington, Indiana 47405, University of Erlangen-Nürnberg, Department of Chemistry and Pharmacy, Inorganic Chemistry, Egerlandstraβe 1, Erlangen, Germany 91058, Nuclear Medicine, Brigham and Women's Hospital, Harvard Medical School, Boston, Massachusetts 02115, Department of Chemistry, RC Box 270216, University of Rochester, Rochester, New York 14627, and Department of Physics and Geology, University of Texas-Pan American, Edinburg, Texas 7854

Received June 19, 2008

One-electron reduction of the square-planar nickel precursor (PNP)NiCl (**1**) (PNP^- = N[2-P($CHMe_2$)$_2$-4-methylphenyl]$_2$) with KC_8 effects ligand reorganization of the pincer ligand to assemble a Ni(I) dimer, [Ni(μ_2-PNP)]$_2$ (**2**), containing a Ni_2N_2 core structure, as inferred by its solid-state X-ray structure. Solution magnetization measurements are consistent with a paramagnetic Ni(I) system likely undergoing a monomer ↔ dimer equilibrium. The room-temperature and 4 K solid-state X-band electron paramagnetic resonance (EPR) spectra display anisotropic signals. Low-temperature solid-state X-band EPR data at 4 K reveal rhombic values $g_z = 1.980(4)$, $g_x = 2.380(4)$, and $g_y = 2.225(4)$, as well as a forbidden signal at $g = 4.24$ for the $\Delta M_S = 2$ half field transition, in accord with **2** having two weakly interacting metal centers. Utilizing an $S = 1$ model, full spin Hamiltonian simulation of the low-temperature EPR spectrum on the solid sample was achieved by applying a nonzero zero-field-splitting parameter ($D = 0.001$ cm^{-1}), which is consistent with an $S = 0$ ground state with a very closely lying $S = 1$ state. Solid-state magnetization data also corroborate well with our solid-state EPR data and reveal weak antiferromagnetic behavior ($J = -1.52(5)$ cm^{-1}) over a 2−300 K temperature range at a field of 1 Tesla. Evidence for **2** being a masked "(PNP)Ni" scaffold originates from its reaction with N_2CPh_2, which traps the Ni(I) monomer in the form of a T-shaped species, Ni(PNP═NNCPh_2), a system that has been structurally characterized. The radical nature of complex **2**, or its monomer component, is well manifested through the plethora of cooperative H−X-type bond cleavage reactions, providing the nickel(II) hydride (PNP)NiH and the corresponding rare functionalities −OH, −OCH_3, −PHPh, and −B(catechol) integrated into the (PNP)Ni moiety in equal molar amounts. In addition to splitting H_2, compound **2** can also engage in homolytic X−X bond cleavage reactions of PhXXPh to form (PNP)Ni(XPh) (X = S or Se).

Introduction

Accessing well-defined Ni(I) complexes is a relatively rare phenomenon given the difficulty in stabilizing this radical and the low-valent oxidation state.[1−9] Despite the paucity of these species, some of the known Ni(I) systems play significant roles in several chemically important processes such as catalytic aliphatic C−C bond formation reactions, and the cyclotrimerization and linear oligomerization of phenyl acetylene.[2] In the catalytic aliphatic C–C coupling reaction, it was noted in the solid state that the Ni(I) centers were not discrete monomers, owing to Ni···Ni interactions.[2b] By the same token, dinuclear Ni(I) cores have also been demonstrated to be important reagents relevant to important industrials processes. For example, dinuclear Ni(I) cores have been used as models for the hydrodesulfurization of sulfur-based heterocycles.[3,4] The

* Authors to whom correspondence should be addressed. E-mail: Karsten.Meyer@chemie.uni-erlangen.de (K.M.), mindiola@indiana.edu (D.J.M.).
[†] Indiana University.
[‡] University of Erlangen-Nürnberg.
[§] Harvard Medical School.
[||] University of Rochester.
[⊥] University of Texas-Pan American.

10.1021/ic801137p CCC: $40.75
Published on Web 10/15/2008

responsible precursor in the process for desulfurization is a bimetallic Ni(I) core bridged by two hydride ligands. Intuitively, to understand the mechanism behind important transformations such as C−C bond formation or desulfurization, it is necessary to determine the electronic structure of the Ni(I) dimeric core, especially since the Ni−Ni interaction appears weak enough to promote redox events possibly via mononuclearity formation. Bimetallic cores consisting of the most accessible oxidation state of Ni, namely, Ni(II) centers, have been scrutinized in depth to address the electronic interaction between the metal ions, more specifically, the mechanism for the communication among the two metal centers via superexchange through spin delocalization or spin polarization.[10] On the contrary, bimetallic centers consisting of Ni(I) ions are a very scarce occurrence and hence lack detailed scrutiny.[3−8] As a result, investigating the electronic and magnetic interactions between two Ni(I) centers should provide clues to how these systems, if any, cooperatively perform important chemical transformations relating to bond-breaking and -forming reactions. In general, understanding the interaction between two metal centers represents an important paradigm in coordination chemistry since it can lead to predictions on how dinuclear moieties operate, in concert and along the way to performing unusual transformations.

In a bimetallic motif consisting of two d^9 metal centers, such as in a Ni(I)/Ni(I) dinuclear complex, one can categorize three different types of electronic states that depend greatly on the strength of metal−metal interactions.[11] In one case, the two metal centers in question can be virtually noninteractive, essentially displaying properties amenable to an isolated d^9 unit and more consistent with a paramagnetic monomer. In a second case scenario, whereby there is weak interaction, the metal centers can be communicating very weakly, thus leading to ferromagnetically and antiferromagnetically coupled ground states, depending on whether the total high-spin or low-spin state is attained. In such a case of weak interaction, it is expected that the triplet excited state should be close in energy to the singlet ground state and that such a low-lying excited state should be populated thermally. In the third case scenario, the two metal centers could be interacting strongly, thereby forming a metal−metal bond which eventually displays diamagnetic behavior. Deciphering these types of interactions can be challenging, given the interplay between metal−metal bonds, ferro- and antiferromagnetic coupling pathways through space or the bridging ligands, and a possible caveat involving a monomer−dimer equilibrium scenario in solution.

In this manuscript, we present a bimetallic system where two Ni(I) centers are assembled in a diamond-like core form, and where the metal ions in question are very weakly interacting despite the connective amido bridges between them. Intuitively, two 17-electron metal centers in proximity and bridged by a strong field ligand such as amido are inclined to interact strongly via the bridge or through space along the way to metal−metal bond formation. Applying X-ray crystallography and other spectroscopic techniques, we elucidate our dinuclear $Ni_2(I,I)$ complex to be a rare and special example of weakly coupled bimetallic framework. Herein, we describe the synthesis of an electronically unusual dinuclear Ni(I) complex, $[Ni(\mu_2\text{-PNP})]_2$, supported by the pincer ligand PNP ($PNP^- = N[2\text{-}P(CHMe_2)_2\text{-}4\text{-methylphenyl}]_2$).[12] Despite having a short Ni···Ni distance, this complex exists at room temperature as a diradical having a Ni_2N_2 diamond core resting state. Although the solution magnetization data suggest this core to equilibrate to two

(1) For some representative Ni(I) complexes: (a) Mindiola, D. J.; Waterman, R.; Jenkins, D. M.; Hillhouse, G. L. *Inorg. Chim. Acta* **2003**, *345*, 299. (b) Ge, P.; Riordan, C. G.; Yap, G. P. A.; Rheingold, A. L. *Inorg. Chem.* **1996**, *35*, 5408. (c) Kieber-Emmons, M. T.; Schenker, R.; Yap, G. P. A.; Brunold, T. C.; Riordan, C. G. *Angew. Chem., Int. Ed.* **2004**, *43*, 6716. (d) Ram, M. S.; Riordan, C. G. *J. Am. Chem. Soc.* **1995**, *117*, 2365. (e) MacBeth, C. E.; Thomas, J. C.; Betley, T. A.; Peters, J. C. *Inorg. Chem.* **2004**, *43*, 4645. (f) Meinhard, D.; Reuter, P.; Rieger, B. *Organometallics* **2007**, *26*, 751. (g) Kandiah, M.; McGrady, G. S.; Decken, A.; Sirsch, P. *Inorg. Chem.* **2005**, *44*, 8650. (h) Bencini, A.; Benelli, C.; Gatteschi, D.; Sacconi, L. *Inorg. Chim. Acta* **1979**, *37*, 195. (i) Bencini, A.; Benelli, C.; Gatteschi, D.; Sacconi, L. *Inorg. Chim. Acta* **1978**, *29*, L243. (j) Dapporto, P.; Sacconi, L. *Inorg. Chim. Acta* **1980**, *39*, 61. (k) Cecconi, F.; Midollini, S.; Orlandini, A. *J. Chem. Soc., Dalton Trans.* **1983**, 2263. (l) Schafer, H.; Binder, D.; Deppisch, B.; Mattern, G. *Z. Anorg. Allg. Chem.* **1987**, *79*, 79. (m) Stavropoulos, P.; Muetterties, M. C.; Carrié, M. M.; Holm, R. H. *J. Am. Chem. Soc.* **1991**, *113*, 8485. (n) James, T. L.; Cai, L. S.; Muetterties, M. C.; Holm, R. H. *Inorg. Chem.* **1996**, *35*, 4148. (o) Scott, F.; Krüger, C.; Betz, P. *J. Organomet. Chem.* **1990**, *387*, 113. (p) Gomez, L.; Pereira, E.; de Castro, B. *J. Chem. Soc., Dalton Trans.* **2000**, 1373. (q) Schebler, P. J.; Mandimutsira, B. S.; Riordan, C. G.; Liable-Sands, L. M.; Incarvito, C. D.; Rheingold, A. L. *J. Am. Chem. Soc.* **2001**, *123*, 331. (r) Mandimutsira, B. S.; Yamarik, J. L.; Brunold, T. C.; Gu, W.; Cramer, S. P.; Riordan, C. G. *J. Am. Chem. Soc.* **2001**, *123*, 9194. (s) Bakac, A.; Espenson, J. H. *J. Am. Chem. Soc.* **1986**, *108*, 713. (t) Sadler, N.; Scott, S. L.; Bakac, A.; Espenson, J. H.; Ram, M. S. *Inorg. Chem.* **1989**, *28*, 3951. (u) Ram, M. S.; Bakac, A.; Espenson, J. H. *Inorg. Chem.* **1986**, *25*, 3267. (v) Barefield, E. K.; Krost, D. A.; Edwards, D. S.; Van Derveer, D. G.; Trytko, R. L.; O'Rear, S. P. *J. Am. Chem. Soc.* **1981**, *103*, 6219. (w) D'Aniello, M. J.; Barefield, E. K. *J. Am. Chem. Soc.* **1978**, *100*, 1474. (x) DeLaet, D. L.; Powell, D. R.; Kubiak, C. P. *Organometallics* **1985**, *4*, 954.

(2) (a) Jones, G. D.; Martin, J. L.; McFarland, C.; Allen, O. R.; Hall, R. E.; Haley, A. D.; Brandon, R. J.; Kanovalova, T.; Desrochers, P. J.; Pulay, P.; Vicic, D. A. *J. Am. Chem. Soc.* **2006**, *128*, 13175. (b) Anderson, T. J.; Jones, G. D.; Vicic, D. A. *J. Am. Chem. Soc.* **2004**, *126*, 8100. (c) Saraev, V. V.; Kraikivskii, P. B.; Vilms, A. I.; Zeliniskii, S. N.; Yunda, A. Y.; Danilovtseva, E. N.; Kuzakov, A. S. *Kinet. Catal.* **2007**, *48*, 778.

(3) Vicic, D. A.; Jones, W. D. *J. Am. Chem. Soc.* **1999**, *121*, 7606.

(4) Vicic, D. A.; Jones, W. D. *J. Am. Chem. Soc.* **1997**, *119*, 10855.

(5) Jonas, K.; Wilke, G. *Angew. Chem., Int. Ed.* **1970**, *9*, 312.

(6) Bach, I.; Goddard, R.; Kopiske, C.; Seevogel, K.; Poerschke, K. R. *Organometallics* **1999**, *18*, 10.

(7) Jonas, K. *J. Organomet. Chem.* **1974**, *78*, 273.

(8) Fryzuk, M. D.; Clentsmith, G. K. B.; Leznoff, D. B.; Rettig, S. J.; Geib, S. J. *Inorg. Chim. Acta* **1997**, *265*, 169.

(9) For examples of three-coordinate Ni(I): (a) Bradley, D. C.; Hursthouse, M. B.; Smallwood, R. J.; Welch, A. J. *J. Chem. Soc., Chem. Commun.* **1972**, 872. (b) Nilges, M. J.; Barefield, E. K.; Belford, R. L.; Davis, P. H. *J. Am. Chem. Soc.* **1977**, *99*, 755. (c) Ellis, D. D.; Spek, A. L. *Acta Crystallogr.* **2000**, *C56*, 1067. (d) Eaborn, C.; Hill, M. S.; Hitchcock, P. B.; Smith, J. D. *Chem. Commun.* **2000**, 691. (e) Mindiola, D. J.; Hillhouse, G. L. *J. Am. Chem. Soc.* **2001**, *123*, 4623. (f) Melenkivitz, R.; Mindiola, D. J.; Hillhouse, G. L. *J. Am. Chem. Soc.* **2002**, *124*, 3846. (g) Kitiachvili, K. D.; Mindiola, D. J.; Hillhouse, G. L. *J. Am. Chem. Soc.* **2004**, *126*, 10554. (h) Kogut, E.; Wiencko, H. L.; Zhang, L.; Cordeau, D. E.; Warren, T. H. *J. Am. Chem. Soc.* **2005**, *127*, 11248. (i) Eckert, N. A.; Dinescu, A.; Cundari, T. R.; Holland, P. L. *Inorg. Chem.* **2005**, *44*, 7702. (j) Wang, H. Y.; Meng, X.; Jin, G. X. *Dalton Trans.* **2006**, 2579. (k) Holland, P. L.; Cundari, T. R.; Perez, L. L.; Eckert, N. A.; Lachicotte, R. J. *J. Am. Chem. Soc.* **2002**, *124*, 14416. (l) Bai, G.; Wei, P.; Stephan, D. W. *Organometallics* **2005**, *24*, 5901. (m) Nilges, M. J.; Barefield, E. K.; Belford, R. L.; Davis, P. H. *J. Am. Chem. Soc.* **1979**, *99*, 755. (n) Hu, X.; Castro-Rodriguez, I.; Meyer, K. *Chem. Comm.* **2004**, 2164–2165.

(10) Arriortua, M. I.; Cortes, A. R.; Lezam, L.; Rojo, T.; Solans, X.; Font-Bardia, M. *Inorg. Chim. Acta* **1990**, *174*, 263.

(11) Hay, P. J.; Thibeault, J. C.; Hoffmann, R. *J. Am. Chem. Soc.* **1975**, *97*, 4884.

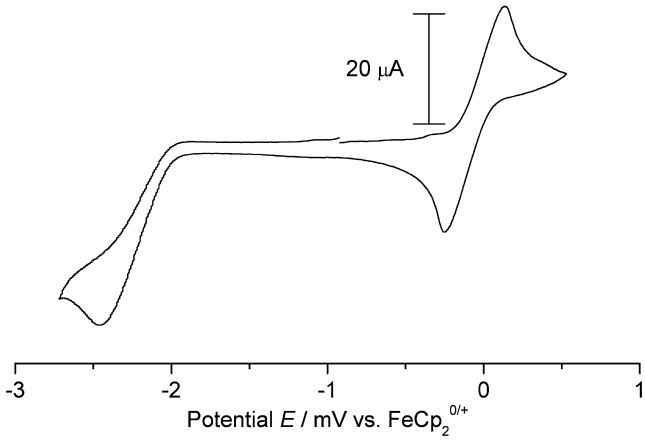

Figure 1. Cyclic voltammagram of **1** in THF using 0.3 M TBAH as an electrolyte and referenced to $Fc^{+/0}$ at 0.0 V. The scan rate is 100 mV/s.

equivalents of the corresponding monomer "(PNP)Ni or solvated form", the dinuclear core along with its paramagnetism is retained in the solid state. Structural analysis of this species confirms that each PNP unit assembling the Ni_2N_2 diamond core slightly differs in geometry. The combination of solid-state magnetization and solid-state electron paramagnetic resonance (EPR) spectroscopic data are in accord with **2** having an accessible $S = 1$ electronic configuration where each Ni radical center weakly antiferromagnetically couples with an overall $S = 0$ ground state and has a $J = -1.52(5)$ cm^{-1} over a 2−300 K range. We also demonstrate that the Ni_2N_2 core is a masked (PNP)Ni(I) surrogate and can undergo binuclear oxidative additions by splitting H−X bonds of various substrates (X = H, OH, OCH_3, PHPh, and B(catechol)), to form equal mixtures of (PNP)Ni−H and (PNP)Ni−X moieties. Some of the latter complexes have been prepared independently and free of hydride. Finally, the solid-state structures for a family of rare, terminal moieties such as (PNP)Ni(OH) and (PNP)Ni(NH_2) are presented and discussed.

Results and Discussion

Synthesis and Solid-State Structure of Complex [Ni(μ_2-PNP)]$_2$ (2). The square-planar complex (PNP)NiCl (**1**) was originally reported by Ozerov and co-workers and can be readily prepared by the addition of (PNP)H to anhydrous $NiCl_2$ in the presence of NEt_3 or by salt metathesis involving (PNP)Li and $NiCl_2(THF)_{1.5}$ (see the Experimental Section).[13] To assess whether compound **1** could be reduced by one electron, we examined its electrochemical behavior in tetrahydrofuran (THF) using a 0.3 M solution of tetrabutylammonium hexafluorophosphate (TBAH) electrolyte in THF. As shown in Figure 1, complex **1** displays a reversible anodic wave close to the $FeCp_2^{0/+}$ redox couple and an irreversible endothermic wave at a potential of −2.48 V. The high reduction potential of **1** suggested that a powerful one-

Scheme 1. Synthesis of Complex **2** via Reduction of **1** with KC_8

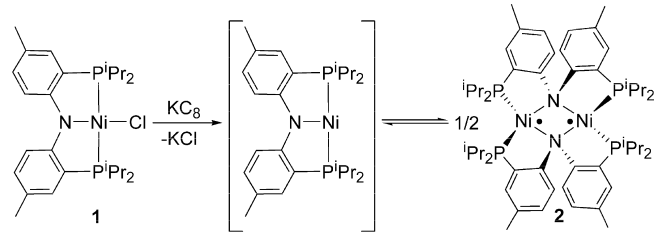

electron reductant should be used,[14] since chemical treatment of **1** with 1% Na/Hg in THF resulted in no detectable reaction when the mixture was assayed by ^1H NMR spectroscopy. However, assembling a reactive Ni(I) species was possible when **1** was treated with 1 equiv of KC_8 in THF, as indicated by an immediate color change from green to dark brown. Upon workup of the mixture, dark crystals of the Ni(I) dimer, [Ni(μ_2-PNP)]$_2$ (**2**), were isolated in 62% yield (Scheme 1). The moderate isolation yield of **2** is due to its high solubility in most common organic solvents as well as the presence of a byproduct, namely, the Ni(II) hydride (PNP)NiH (**3**) (5−15% yield based on ^1H NMR spectra having an internal standard). Complex **3** has been previously reported by Ozerov and co-workers and displays a diagnostic hydride resonance at −18.4 ppm ($J_{H-P} = 60$ Hz).[13] Fortunately, we found that the complex can be obtained in very pure form, and in reproducible yields, when **1** is subjected to freshly prepared KC_8. In addition, the separation of **2** from traces of **3** can be achieved by fractional crystallization of the mixture at −35 °C using hexane as solvent. Independently, we have found that the treatment of **2** with excess KC_8 in THF does not produce **3** (no reaction), suggesting that the over-reduction (if occurring) of Ni(I) is not a competing process. Notably, the origin of the hydride ligand in **3** was not from the solvent medium, THF, since the treatment of **2** with 1 equiv of KC_8 in THF-d_8 did not yield the expected isotopologue (PNP)NiD (**3**)-d_1 (likewise, **3** + KC_8 does not yield **2** and KH). Therefore, these results advocate that **2** is not a precursor to **3** and that the hydride must originates from ligand degradation of the pincer ancillary in **1** or from a byproduct or impurity originated from KC_8.

The formation of **2** is likely occurring via a transient three-coordinate Ni(I) putative species,[9] "(PNP)Ni" (Scheme 1), which subsequently dimerizes by substantial reorganization of the PNP pincer framework. The degree of aggregation and rearrangement of the former pincer-type ligand is inferred by single-crystal X-ray diffraction analysis (XRD; Figure 2, top) and clearly portrays a Ni_2N_2 diamond core framework whereby the PNP ancillary is severely reorganized via bridging of the pincer amide nitrogen. The bottom of Figure 2 emphasizes the first coordination sphere comprising the diamond core in the solid state structure of **2**. Congruently, the phosphorus atoms composing a PNP ligand extend across each metal center. This expansion of the phosphine pendant arm adds some strain to the aryl framework, which is reflected by the dihedral angles N−C−C−P (1.4(4), 1.8(4), 6.2(4), and 6.8(4)°). Therefore, this discrepancy in dihedral angles implies

(12) (a) Fan, L.; Foxman, B. M.; Ozerov, O. V. *Organometallics* **2004**, *23*, 326. (b) Fan, L.; Yang, L.; Guo, C.; Foxman, B. M.; Ozerov, O. V. *Organometallics* **2004**, *23*, 4778. (c) Ozerov, O. V.; Guo, C.; Papkov, V. A.; Foxman, B. M. *J. Am. Chem. Soc.* **2004**, *126*, 4792.

(13) Ozerov, O. V.; Guo, C.; Fan, L.; Foxman, B. M. *Organometallics* **2004**, *23*, 5573.

(14) Connelly, N. G.; Geiger, W. E. *Chem. Rev.* **1996**, *96*, 877.

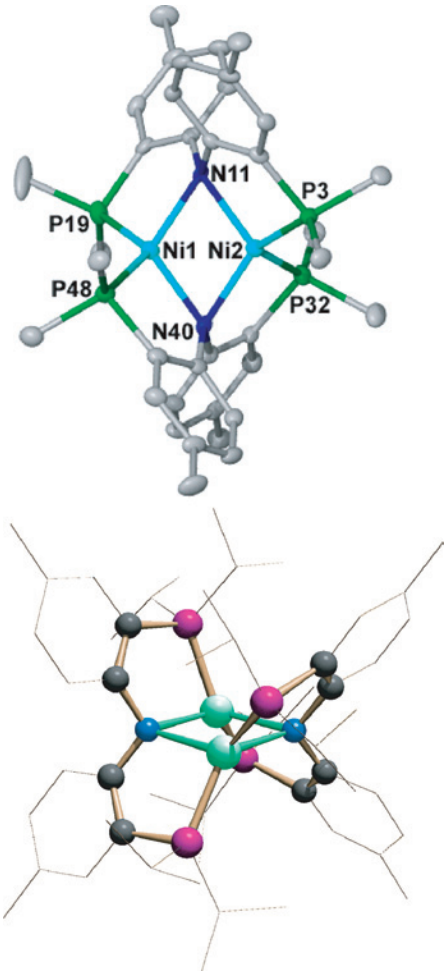

Figure 2. Molecular structure of **2** (top) depicting thermal ellipsoids at the 50% probability level with H atoms, the Et_2O molecule, and isopropyl methyls omitted for clarity. The bottom figure emphasizes the Ni_2N_2 core along with the bridging phosphines. Selected metrical parameters are reported in angstroms and degrees. Ni(1)−Ni(2), 2.3288(7); Ni(1)−N(11), 2.050(3); Ni(1)−N(40), 2.084(3); Ni(1)−P(48), 2.2138(10); Ni(1)−P(19), 2.2195(10); Ni(2)−N(11), 2.062(3); Ni(2)−N(40), 2.070(3); Ni(2)−P(32), 2.2287(10); Ni(2)−P(3), 2.2344(10); P(19)−Ni(1)−P(48), 122.17(4); P(32)−Ni(2)−P(3), 119.30(4); Ni(1)−N(11)−Ni(2), 68.99(9); Ni(1)−N(40)−Ni(2), 68.19(9); N(11)−Ni(1)−N(40), 111.33(11); N(11)−Ni(2)−N(40), 111.43(11); N(11)−Ni(1)−P(19), 89.64(8); N(11)−Ni(1)−P(48), 126.00(8); N(11)−Ni(2)−P(3), 89.09(8); N(11)−Ni(2)−P(32), 124.66(8); N(40)−Ni(1)−P(19), 120.72(8); N(40)−Ni(1)−P(48), 89.72(8); N(40)−Ni(2)−P(3), 127.51(8); N(40)−Ni(2)−P(32), 88.63(8).

that one PNP ligand in **2** is undergoing more tension than the other, and that each half of the molecule is not strictly equivalent. Likewise, the C−N−C−C angles (42.5 (4), 42.6 (4), 44.5 (4), and 47.7(4)°) also depict a considerable amount of torsion involved in the ligand framework. The angles between two aryl rings connected to nitrogen are 74.07(11) and 72.45(11)°, respectively, which might be the result of strain. As a result of these torsions, the molecule cannot possess an inversion center, despite each Ni environment and its first coordination sphere being grossly identical. Although the Ni_2N_2 diamond core appears symmetrical at first sight (Figure 2), closer inspection of other salient metrical parameters exposes subtle differences in the Ni−P distances (Ni(1)−P(19), 2.2195(10); Ni(1)−P(48), 2.2138(10) vs Ni(2)−P(3), 2.2344(10); Ni(2)−P(32), 2.2287(10) Å) and Ni−N distances (Ni(1)−N(11), 2.050 (3); Ni(1)−N(40), 2.084 (3) vs Ni(2)−N(11), 2.062 (3); Ni(2)−N(40), 2.070(3) Å), thus hinting that each metal center is experiencing a slightly different chemical environment. Given the acute Ni−N−Ni angles, each metal center is proximal, having a distance of 2.3288(7) Å between them (Figure 2). Other notable metrical parameters for **2** are listed with Figure 2. An analogous geometry to **2** has been recently reported for Co(I)[15] and Cu(I)[16] systems bearing a similar PNP ligand. The diamond core structure presented here does differ significantly from a Ag(I) dimeric structure formed with this same PNP ligand.[17]

Magnetism of Complex 2. Logically, the radical nature of each Ni(I) (formally 17 valence electrons per Ni center) should be quenched, per se, via the formation of a Ni···Ni bond, a metrical parameter which is extremely short in our case, 2.3288(7) Å (vide supra). Considering the short Ni···Ni distance found in **2**, a strong antiferromagnetic interaction between the centers was anticipated, which would therefore result in an overall diamagnetic ground state for **2**. A similar coupling phenomenon has been observed in the case of the hydride dimers $[(^tBu_2P)_2CH_2CH_2)Ni]_2(\mu_2\text{-}H)_2$ and $[((^iPr_2P)_2\text{-}CH_2CH_2CH_2)Ni]_2(\mu_2\text{-}H)_2$ where the Ni−Ni distances are in fact slightly longer at 2.433(1) (structure severely disordered) and 2.438(1) Å, respectively.[6,18] Despite having a very short Ni···Ni distance, a value comparable with the calculated covalent radii (2.33 Å),[19] compound **2** was found to be paramagnetic. The magnetic moment, μ_{eff}, of a solution of **2** (calculated for the monomer), measured by the Evans method, was determined to be $1.78(1)\mu_B$ at 25 °C in toluene. The magnetic moment is slightly temperature-dependent, varying from 1.45 μ_B at 218 K to 1.74 μ_B at 348 K, suggesting that **2** might exist as a mixture of monomers "(PNP)Ni, (PNP)Ni(solvent)", and a dinuclear compound.[20] The same magnetic behavior has been observed in pyridine but not in cyclohexane, thus implying that **2** might be undergoing a ligand rearrangement in coordinating solvents.[20] A similar equilibrium scenario has been proposed for the Co(I) analogue, $[Co(\mu_2\text{-PNP})]_2$, recently reported by our group.[15] However, given our inability to identify the species present in solution, we studied the magnetism of microcrystalline solid samples of **2**. This feature would also allow for an analysis and direct comparison with the solid-state structure, as determined by XRD (vide supra).

The magnetizations of crystalline samples of **2** were measured by SQuID magnetometry in the temperature range between 2 and 300 K at a field of 1 Tesla. The data were

(15) Fout, A. R.; Basuli, F.; Fan, H.; Tomaszewski, J.; Huffman, J. C.; Baik, M.-H.; Mindiola, D. J. *Angew. Chem., Int. Ed.* **2006**, *45*, 3291.
(16) (a) Harkins, S. B.; Peters, J. C. *J. Am. Chem. Soc.* **2005**, *127*, 2030. (b) Mankad, N. P.; Rivard, E.; Harkins, S. B.; Peters, J. C. *J. Am. Chem. Soc.* **2005**, *127*, 16032. (c) Harkins, S. B.; Mankad, N. P.; Miller, A. J. M.; Szilagyi, R. K.; Peters, J. C. *J. Am. Chem. Soc.* **2008**, *130*, 3478. (d) Harkins, S. B.; Peters, J. C. *J. Am. Chem. Soc.* **2004**, *126*, 2885.
(17) DeMott, J. C.; Basuli, F.; Kilgore, U. J.; Foxman, B. M.; Huffman, J. C.; Ozerov, O. V.; Mindiola, D. J. *Inorg. Chem.* **2007**, *46*, 6271.
(18) Fryzuk, M. D.; Clentsmith, G. K. B.; Leznoff, D. B.; Rettig, S. J.; Geib, S. J. *Inorg. Chim. Acta* **1997**, *265*, 169.
(19) Pauling, L.; *The Nature of Chemical Bond*; Cornell University Press: Ithaca, NY, 1939.
(20) See the Supporting Information.

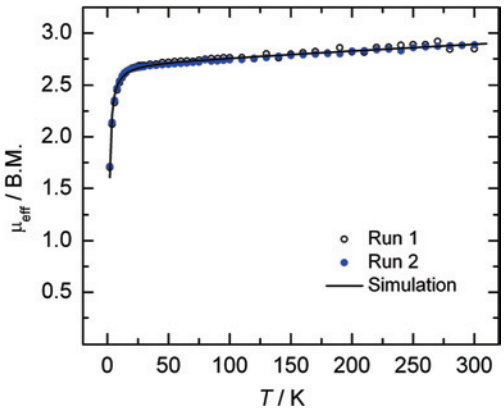

Figure 3. Plot of μ_{eff} as a function of temperature shown for **2** in the temperature interval 2−300 K. Open spheres and blue spheres represent runs performed on two independently prepared samples. The line shows the fit using the dimer model and the parameters described in the text.

corrected for underlying diamagnetism using tabulated Pascals constants[21] and plotted as the effective magnetic moment versus temperature (Figure 3). The effective magnetic moment varies from 1.6 μ_B at 2 K to 2.9 μ_B at 300 K. Disregarding a temperature-independent paramagnetism (TIP) of 450 × 10^{-6} $cm^3 \cdot mol^{-1}$ per dimer molecule, the susceptibility is fairly constant over the temperature interval 50−300 K. This data was reproducible with an independently prepared sample of microcrystalline **2** (referred to, in Figure 3, as Run 2).

Qualitatively, the magnetization data of **2** could correspond to three different situations. Case 1 is a very strong ferromagnetic coupling between the $S = 1/2$ nickel centers with a triplet ground state ($S_{total} = 1$) and an exited singlet state ($S_{total} = 0$), which is not partially populated even at room temperature (>500 cm^{-1} higher in energy). Case 2 corresponds to magnetically isolated $S = 1/2$ centers, while case 3 is a weakly antiferromagnetically coupled dimer with a singlet ground state and an excited triplet state only several cm^{-1} higher in energy.

In order to address the most logical case for **2**, the experimental data were fitted to all three cases using the appropriate spin Hamiltonian. In each case, there is a gradual decrease of the effective magnetic moment at very low temperatures. In cases 1 and 2, the latter feature will be due to intermolecular interactions with neighboring nickel centers and is expressed as a Weiss temperature, while in case 3, this lowering in effective magnetic moment is mainly due to the intramolecular antiferromagnetic interaction in the dimer.

Our best fit is case 3 and is displayed in Figure 3 as a solid black line. The model used is a dimer model using the usual spin Hamiltonian $H = -2J(S_1 \times S_2) + g\mu_B B(S_1 + S_2)$ with $S_1 = S_2 = 1/2$. The parameters found are a small coupling component $J = -1.52(5)$ cm^{-1}, an isotropic g value of 2.21(1), a TIP of 450 × 10^{-6} $cm^3 \cdot mol^{-1}$, and a Weiss temperature of $\theta = -0.4$ K. The g value is in excellent agreement with the g values obtained from solution and solid-state EPR data (2.205 and 2.214, vide infra).

On the grounds of our SQuID data, case 1 is discarded since the g value obtained in this fit (1.95) deviates significantly from the one found by EPR spectroscopy (vide infra). We also find it unlikely to observe such an extremely strong ferromagnetic coupling regardless of the Ni−Ni distance. In the case of isoelectronic Cu(II) dimers, no documented cases having a ferromagnetic coupling to even a third of this magnitude have been experimentally observed.[16] Case 2 is less easily discarded, and we disfavor the uncoupled model on the basis of the fit of the magnetization data in conjunction with the solid-state X-band EPR spectroscopic data (vide infra).

X-Band EPR Spectroscopy of Complex 2. EPR spectra of compound **2** were simulated using the spin Hamiltonian $H = \mu_B g_x S_x B_x + \mu_B g_y S_y B_y + \mu_B g_z S_z B_z + D(S_z^2 - 1/3S(S + 1))$. The X-band EPR spectrum of **2** recorded in toluene solution at room temperature (298 K) shows a virtually featureless single resonance line that can be simulated with an isotropic g value of 2.205(5) (Figure S5, Supporting Information). However, the X-band EPR performed on **2** in the solid state displays an anisotropic rhombic signal at 298 K (Figure 4, top). The spectrum was simulated using three different g values of 2.393(4), 2.238(4), and 1.992(4). The average of the anisotropic g values is 2.214(4) and within the uncertainty; this is the same as the isotropic value measured in solution, indicating that both the solution and solid-state EPR signals originate from the same species. We cannot refute, however, whether the solution spectrum is a superposition of dimer and monomer spectra, especially if they have similar g values. The g values observed for complex **2** are analogous to that found by others.[22b] The nonaxiality of the coordination environment for the nickel centers (Figure 2) is clearly reflected in the rhombic anisotropy of the experimental g values.

As discussed earlier, magnetization data have shown that the Ni(I) centers are weakly antiferromagnetically coupled, and this observation prompted us to corroborate these findings by performing low-temperature EPR spectroscopy. Accordingly, the solid-state spectrum of **2** at 4 K is shown in Figure 4 (middle). The spectroscopic features are very similar to the room-temperature spectra but with slightly lower g values of 2.380(4), 2.225(4), and 1.980(4).

On the basis of magnetization and EPR data, we wish to distinguish between case 2 and case 3 (vide supra). The main lines in the solid-state EPR spectrum of complex **2** were simulated using both models (Figure 4, top and middle). A low-intensity feature at approximately half field (positioned at $g = 4.24$) was observed at 4 K, and this feature should only be present in case 3: a weak interaction in a dinuclear complex (Figure 4, bottom).[22] The red lines in Figure 4 display the simulations using the dimer model: a spin Hamiltonian with $S = 1$. At 4 K: $S = 1$, $g_x = 2.380(4)$, $g_y = 2.225(4,)$, $g_z = 1.980(4)$, $D = 0.001$ cm^{-1}, line width =

(21) (a) O'Connor, C. J. *Prog. Inorg. Chem.* **1982**, *29*, 203. (b) David, R. L. *CRC Handbook of Chemistry and Physics*, 60th ed.; CRC Press: Boca Raton, FL, 1979.

(22) (a) Meyer, K.; Bendix, J.; Bill, E.; Weyhermuller, T.; Wieghardt, K. *Inorg. Chem.* **1998**, *37*, 5180. (b) Muresan, N.; Weyhermüller, T.; Wieghardt, K. *Dalton Trans.* **2007**, 4390.

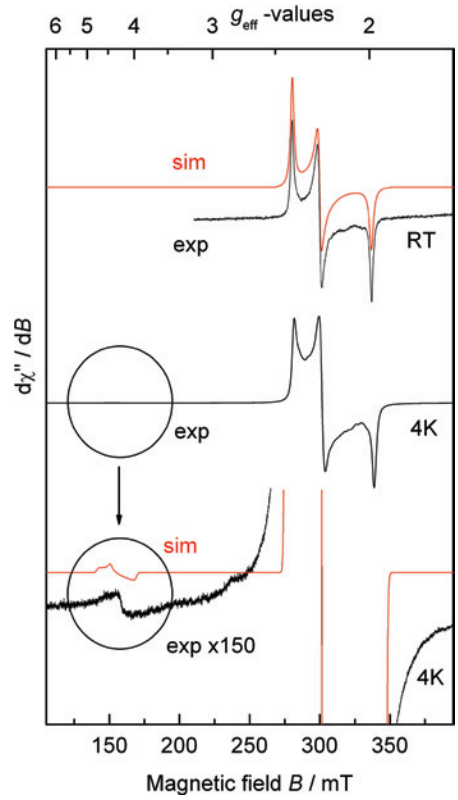

Figure 4. X-band EPR spectra of solid state **2** at room temperature (top) and at 4 K (middle). At the bottom, the 4 K spectra has been expanded by a factor of 150 to show the weak line found at approximately half field (g value of the position of this line is 4.24). Experimental conditions at 300 K: microwave frequency, 9.390083 GHz; microwave power, 0.2012 mW; modulation frequency, 100 kHz; modulation amplitude, 0.8 mT. At 4 K, middle spectrum: microwave frequency, 9.016023 GHz; microwave power, 0.998 mW; modulation frequency, 100 kHz; modulation amplitude, 1.0 mT. At 4 K, bottom spectrum: microwave frequency, 9.014827 GHz; microwave power, 0.998 mW; modulation frequency, 100 kHz; modulation amplitude, 0.5 mT, collected over three runs. The simulations shown as red lines were performed with the spin Hamiltonian model and the parameters described in the text. The field scales of the middle and bottom spectra have been corrected for the differing frequencies compared to the top spectrum to facilitate comparisons.

25 G, and Lorentzian line shapes. At 25 °C: $S = 1$, $g_x = 2.393(4)$, $g_y = 2.238(4)$, $g_z = 1.992(4)$, $D = 0.000$ cm^{-1}, line width = 17 G, and Lorentzian line shapes. We have also recorded a series of solution EPR spectra in the temperature range 280−175 K and found that the intensity of the $g = 2.205$ signal decreases gradually upon lowering the temperature, thus consistent with a diamagnetic $S = 0$ ground state being populated over the $S = 1$ low-lying excited state.[22a] The presence of a small nonzero zero-field-splitting parameter, D, in the spin Hamiltonian will induce a slight mixing of the three energy levels in the triplet state ($M_S = -1$, 0, and +1), and this will relax the selection rules, therefore inducing intensity in the forbidden $\Delta M_S = 2$ line found at the half-field signal ($g = 4.24$) in our simulation. The observed experimental line is more than a magnitude stronger than the simulated line, and we tentatively assign this to the fact that the nickel centers are not truly equal. This is in fact the case when examining the solid-state structure of **2** (vide supra). It has been demonstrated that lowering the symmetry of the system is very effective in increasing intensity in the forbidden line.[23] We do not have

Scheme 2. Synthesis of Complex **4** from **2** and 2 equiv of N_2CPh_2

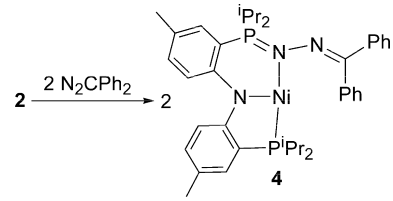

enough evidence, however, to unambiguously determine the magnitude or main axis of the zero-field-splitting and can only therefore confirm this parameter to indeed be nonzero at liquid helium temperatures, and that it is maximally at 0.0015 cm^{-1}. Otherwise, splitting in the main lines would be present, which we do not observe in our case. Due to the anisotropy in the g values, the position of the half-field line is dependent on which g value is assigned to the z axis. Our findings point toward the lower g value being assigned to the z axis (axis of the zero-field splitting parameter D).

It is noted that we did not observe the weak half-field line in background measurements. It is unlikely that a decomposition/impurity byproduct of **2** would be responsible for this signal given our consistent magnetization data collected for two independently crystallized samples. Although extremely small amounts of iron(III) impurities can generate a weak signal at 4.3 K, we are confident that compound **2** is analytically pure material which is prepared under highly reducing conditions. Hence, the plausibility of an iron(III) impurity present in the final product is unlikely, especially if the data are reproducible with independently prepared samples of crystalline **2**.

Trapping of the Ni(I) Monomer. Despite our definitive evidence for **2** being a diradical species in the solid state both at room temperature and near absolute zero, the possibility of such species dissociating into the corresponding monomer, in solution, is still questionable. The results obtained by Evans, although inconclusive, do indeed suggest that a monomer ↔ dimer equilibrium could be operative in **2**, since its magnetization measurements slightly varied over a temperature range and depend on the nature of the solvent medium (vide supra). Gas chromatography−mass spectrometry measurements also suggested that the dimeric core in **2** was fragile enough to break into its corresponding monomers (calcd, 486.1989; found, 486.1977). However, the most conclusive proof for the formation of a monomer in solution stems from molecular weight measurements obtained by the freezing point depression method of a 1.0% w/w solution of **2** in naphthalene at its melting point.[24] The average observed value collected on four different samples, 379(107) g/mol, is lower than the expected value for the monomer but within the limitation of the method (see the Experimental Section). Therefore, these results imply that **2** is mostly a monomer near the melting point of naphthalene (~80 °C). Despite unsuccessful attempts to trap the elusive three-coordinate Ni(I) species with donors such as THF, $P(CH_3)_3$, and pyridine, the treatment of **2** with 2 equiv of N_2CPh_2 resulted

(23) Abragam, A.; Bleaney, B. *Electron Paramagnetic Resonance of Transition Ions*; Clarendon Press: Oxford, U.K., 1970.
(24) Smith, J. M.; Lachicotte, R. J.; Holland, P. L. *J. Am. Chem. Soc.* **2003**, *125*, 15752.

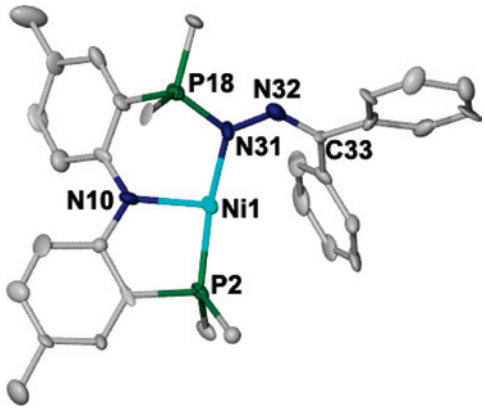

Figure 5. Molecular structure of **4** depicting thermal ellipsoids at the 50% probability level with H atoms, the Et_2O molecule, and isopropyl methyls omitted for clarity. Selected metrical parameters are reported in angstroms and degrees. Ni(1)−N(31), 1.913(8); Ni(1)−N(10), 1.979(9); Ni(1)−P(2), 2.158(3); P(18)−N(31), 1.678(8); N(31)−N(32), 1.408(10); N(31)−Ni(1)−N(10), 98.5(3); N(31)−Ni(1)−P(2), 165.7(3); N(10)−Ni(1)−P(2), 88.4(3); P(18)−N(31)−Ni(1), 115.2(4); N(32)−N(31)−P(18), 108.5(7); N(32)−N(31)−Ni(1), 125.8(7); C(33)−N(32)−N(31), 114.4(9).

in a gradual color change from dark to brown concurrent with precipitation of the three-coordinate Ni(I) complex Ni(PNP═NNCPh$_2$) (**4**) as a brown solid (Scheme 2). Complex **4** is a paramagnetic Ni(I) species (μ_{eff} = 2.22(3) μ_B) and, therefore, shows a broad isotropic X-band EPR signal at g_{iso} = 2.19 (Figure S6, Supporting Information).[20] The line is probably broadened (line width, W = 55 G) due to unresolved hyperfine coupling with proximal nuclear spins such as ^{31}P (I = 1/2) and ^{14}N (I = 1).

To determine the geometry at the metal center and confirm the degree of aggregation in **4**, we resorted to XRD studies. Accordingly, the molecular structure of **4** reveals a T-shaped Ni(I) center[9] in which one of the pendant phosphorus arms composing the PNP framework has been oxidized by the diazo unit to furnish a mono-substituted (phosphoranylidene)-hydrazone group (PNP═NNCPh$_2$). The α-*N* of the (phosphoranylidene)hydrazone moiety is bound to the nickel center (Figure 5). Ylide bond formation (N═P distance is 1.678(8) Å) results via the coordination of this nucleophilic site to the Ni(I) center (Ni−N, 1.913(8) Å), a parameter comparable to the Ni−N$_{amide}$ distance of 1.979(9) Å obtained for the pincer amide group. Coincidently, one of the phenyl groups from the former diazo reagent blocks the open coordination site of the Ni(I) ion, but the closest Ni···C distance is too far to be considered a significant interaction (>2.92 Å). Although complex **4** represents a "trapped" version of the Ni(I) monomer in **2**, the formation of this complex still casts some doubt as to whether this species was generated from the monomer or dimer. Given the sterically congested environment in **2**, however, it thus seems logical to propose that **4** originates from the reaction of N_2CPh_2 with a putative "(PNP)Ni" monomer in solution.

Reductive Bond Splitting Reactions Promoted by Complex 2. The radical nature of **2** allows this species to behave as a two-electron reductant with each nickel center acting as a masked three-coordinate "(PNP)Ni" source. As a result, the treatment of **2** with substrates such as H−X (X = H, OH, OCH_3, PHPh, B(catechol)) immediately leads to splitting of the H−X bond concurrent with formation of an equal mixture of Ni(II) products (PNP)NiH[13] and (PNP)NiX (X = H[13] (**3**), OH (**5**), OCH_3 (**6**), PHPh (**7**), and the boryl B(catechol) (**8**)) according to Scheme 3. The identities of **3** and **5**−**7** have been confirmed independently by the salt metathesis of **1** with the appropriate MX reagent (M = Na, X = BH_4;[13] M = K, X = OH; M = Na, X = OCH_3; M = Li, X = PHPh; Scheme 3). With the exception of **5**, the transmetalation of **1** with X^- is very clean, if not quantitative. The identity of **3** was compared to independently prepared samples originally reported by Ozerov and co-workers.[13] The formation of hydride-free **8** on the other hand was achieved by the addition of biscatecholdiborane ((catechol)$_2B_2$) to **2** (Scheme 3), a process that involves an unprecedented B−B bond cleavage promoted by two Ni(I) centers. Analogous to **3**, the ^{31}P and ^{13}C NMR spectra for **5**−**8** display resonances consistent with square-planar Ni(II) environments, while the ^{1}H NMR spectra reveal diagnostic resonances for the terminal hydroxyl (−5.06 ppm, $^3J_{H-P}$ = 6 Hz), methoxide (3.30 ppm), and phenylphosphide (doublet of triplets, 3.64 ppm, $^1J_{H-P}$ = 179 Hz and $^3J_{H-P}$ = 20 Hz). In the case of compound **8**, the

Scheme 3. Bond Splitting Reactions Involving **2** and Independent Routes to Forming Complexes **3**, **5**−**8**

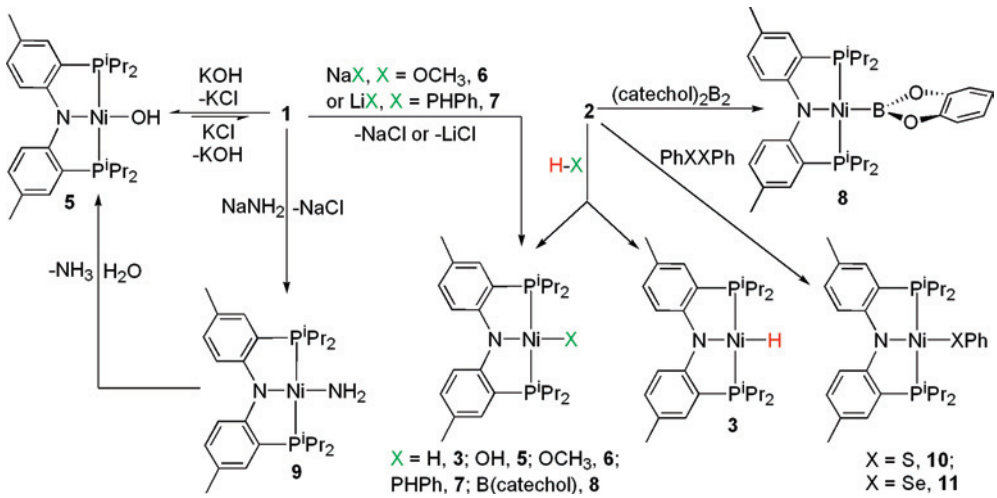

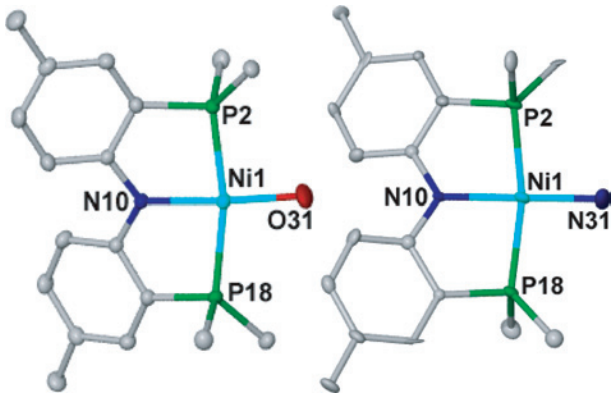

Figure 6. Molecular structures of **5** (left) and **9** depicting thermal ellipsoids at the 50% probability level with H atoms, solvent molecules, and isopropyl methyls omitted for clarity. Selected metrical parameters are listed in Table 1.

^{11}B NMR spectrum clearly reveals the formation of a rare example of a nickel-boryl (~47 ppm). Complex **8** can be also independently prepared via treatment of **3** with catecholborane,[25] and its solid-state structure has been also recently reported by us.[25]

As noted before, the formation of **5** via salt metathesis was not quantitative given the presence of water and soluble Cl^- to regenerate **1** (Scheme 3). The presence of a large excess of KOH modestly improved the formation of **5** and suggested that an equilibrium scenario was hampering the generation of pure **5**. However, in the course of finding a better leaving group, we discovered that H_2O cleanly reacts with (PNP)Ni(NH_2) (**9**), prepared readily from **1** and $NaNH_2$ in THF, to extrude NH_3 concomitant with the formation of **5** (Scheme 3). Attempts to generate **9** from a binuclear oxidative addition of NH_3 to **2**[26] resulted in only the formation of an equal molar amount of **3** and **5**. Despite extensive attempts to generate an anhydrous NH_3 reagent, the formation of **3** and **5** was unavoidable, possibly due to adventitious H_2O.

Given the rarity of terminal Ni(II) hydroxyls, and parent amides,[27,28] we proceeded to collect solid-state structural data for **5** and **9**. As indicated in Figure 6, the crystal structure for each displays square-planar Ni(II) systems bearing terminal −OH and $-NH_2$ functionalities, respectively. The Ni−O (1.8634(9) Å) and Ni−N (1.884(9) Å) distances in **5** and **9** are comparable to the few examples of crystallographically characterized terminal nickel amides, 1.872(2) Å,[27a] and hydroxides, 1.865(17),[27b] 1.877(4),[27c] and 1.955(2)[28] Å. A comparison of the metrical parameters between **5** and **9** is reported in Table 1.

Table 1. Selected Metrical Parameters for the Molecular Structures of **5** and **9**[a]

	5	**9**
Ni−X	1.8634(9)	1.884(9)
Ni−P	2.1883(4), 2.2025(4)	2.192(4), 2.195(4)
Ni−N	1.9125(8)	1.931(7)
P−Ni−P	167.986(11)	167.79(10)
N−Ni−P	84.13(3), 83.98(2)	84.0(3), 84.0(3)
P−Ni−X	92.39(3), 99.50(3)	96.1(4), 95.9(4)
N−Ni−X	176.52(4)	179.3(6)
$Ni_{deviation}$	0.016	0.014

[a] Metrical parameters reported in angstroms and degrees, where X^- represents OH for complex **5** and NH_2 for complex **9**.

In addition to H_2, complex **2** can engage in other homolytic bond-splitting reactions since the addition of 1 equiv of PhXXPh smoothly oxidizes the Ni_2(I,I) core to the corresponding square-planar complexes (PNP)Ni(XPh) (X = S, **10**; X = Se, **11**; Scheme 3) quantitatively. The most notable spectroscopic feature for compounds **10** and **11** includes the observation of a C_2 symmetric system (^{31}P NMR: 33.6 and 36.4 ppm, respectively). Riordan et al.[29] have reported S−S reductive bond cleavage reactions of elemental sulfur by Ni(I) centers, while Hillhouse et al.[1a] have reported a similar reaction to ours: reductive cleavage of the S−S bond in PhSSPh by a dimeric Ni(I) complex.

Conclusions

X-ray, magnetization, and EPR data corroborate well with the Ni_2N_2 unit in **2**, having two unpaired electrons in an overall $S = 0$ ground state with reachable $S = 1$, where the nickel centers are not isolated. The unpaired electrons do couple, but this interaction is weak and occurs at lower temperatures (< 50 K). The possibility of **2** undergoing a monomer ↔ dimer equilibrium in solution should not be refuted, given the findings of molecular weight determination in solution along with our ability to trap a Ni(I) monomer with substrates such as N_2CPh_2. Our results present compelling evidence to suggest that a dinuclear Ni(I) radical-based system possessing a Ni_2N_2 diamond core resting state can engage in H−X splitting reactions.[30] The two Ni(I) centers in **2** appear to be reducing these substrates in concert and in a manner in accord with a binuclear oxidative addition,[30] since no H_2 has been detected for the aforementioned reactions. However, we cannot rule out the possibility of the PNP framework in **2** rearranging, in the presence of substrates, to a metal−metal bonded species, (PNP)Ni−Ni(PNP). Regardless of the mechanism, complex **2** reacts analogously to a Pd analogue recently reported by Ozerov and co-workers.[26a] The dissociation of **2** into its corresponding monomers, "(PNP)Ni", and promotion of a radical chain reaction could also be operative, analogous to well docu-

(25) Adhikari, D.; Huffman, J. C.; Mindiola, D. J. *Chem. Commun.* **2007**, 4489.
(26) (a) Fafard, C. M.; Adhikari, D.; Foxman, B. M.; Mindiola, D. J.; Ozerov, O. V. *J. Am. Chem. Soc.* **2007**, *129*, 10318. Oxidative addition of NH_3 at a single metal center has been also reported. (b) Zhao, J.; Goldman, A. S.; Hartwig, J. F. *Science* **2005**, *307*, 1080.
(27) (a) Campora, J.; Palma, P.; del Rio, D.; Conejo, M. M.; Alvarez, E. *Organometallics* **2004**, *23*, 5653. (b) Campora, J.; Palma, P.; del Rio, D.; Alvarez, E. *Organometallics* **2004**, *23*, 1652. (c) Campora, J.; Matas, I.; Palma, P.; Graiff, C.; Tiripicchio, A. *Organometallics* **2005**, *24*, 2827. (d) Siegfried, L.; Kaden, T. A.; Meyer, F.; Kircher, P.; Pritzkow, H. *Dalton Trans.* **2001**, *15*, 2310. (e) Meyer, F.; Kaifer, E.; Kircher, P.; Heinze, K.; Pritzkow, H. *Chem.—Eur. J.* **1999**, *5*, 1617.
(28) Kieber-Emmons, M. T.; Schenker, R.; Yap, G. P. A.; Brunold, T. C.; Riordan, C. G. *Angew, Chem., Int. Ed.* **2004**, *43*, 6716.
(29) Cho, J.; Van Heuvelen, K. M.; Yap, G. P. A.; Brunold, T. C.; Riordan, C. G. *Inorg. Chem.* **2008**, *47*, 3931.
(30) (a) Crabtree, R. H. *The Organometallic Chemistry of the Transition Metals*; Wiley Interscience: New York, 2001. (b) Jamali, S.; Nabavizadeh, S. M.; Rashidi, M. *Inorg. Chem.* **2005**, *44*, 8594. (c) Cui, W.; Zhang, P. X.; Wayland, B. B. *J. Am. Chem. Soc.* **2003**, *125*, 4994. (d) Jimenez, M. V.; Sola, E.; Lopez, J. A.; Lahoz, F. J.; Oro, L. A. *Chem.—Eur. J.* **1998**, *4*, 1398.

mented cases such as $[Co(CN)_5]^{3-}$, and other metal radicals such as Rh(II), and mixed valent Ir_2 cores.[30,31] Given the ability of **2** to generate unusual terminal groups on nickel(II) presumably by homolytic and heterolytic bond cleavage processes, we are currently exploring other substrates prone to two-electron reduction reactions, since this will allow us to assemble other rare functional groups onto nickel for subsequent group-transfer chemistry. Since **2** presents a special and rare example of a very weakly coupled bimetallic Ni(I) system, the underlying reason behind this uncoupled behavior as well as the mechanism for antiferromagnetic coupling will be interesting aspects to investigate. The governing factors behind such a weakly coupled behavior in **2**, as well as the mechanistic detail of the bond cleavage reactions promoted by the $Ni_2(I,I)$ core, are currently being studied in our laboratories.

Experimental Section

General Procedures. Unless otherwise stated, all operations were performed in an M. Braun Laboratory Master double-dry box under an atmosphere of purified nitrogen or using high-vacuum standard Schlenk techniques under an argon or dinitrogen atmosphere. Anhydrous *n*-hexane, pentane, toluene, and benzene were purchased from Aldrich in sure-sealed reservoirs (18 L) and dried by passage through two columns of activated alumina and a Q-5 column.[32] Diethylether was dried by passage through a column of activated alumina.[32] THF was distilled, under nitrogen, from purple sodium benzophenone ketyl and stored under sodium metal. Distilled THF was transferred under vacuum into a thick-walled reaction vessels before being carried into a dry box. Deuterobenzene was purchased from Cambridge Isotope Laboratory, degassed, and vacuum-transferred to 4 Å molecular sieves. All other deuteron solvents were stored under sodium metal. Celite, alumina, and 4 Å molecular sieves were activated under vacuum for overnight at 200 °C. $NiCl_2(THF)_{1.5}$,[33] (PNP)H,[12] Li(PNP),[12] KC_8,[34] Ph_2CN_2,[35] and LiPHPh[36] were prepared according to the literature methods. All other chemicals were purchased from Strem Chemicals or Aldrich and used as received. CHN analyses were performed by Desert Analytics, Tucson, Arizona. ^1H, ^{13}C, ^{11}B, and ^{31}P NMR spectra were recorded on Varian 500, 400, or 300 MHz NMR spectrometers. ^1H and ^{13}C NMR are reported with reference to residual solvent resonances. ^{31}P NMR chemical shifts are reported with respect to external H_3PO_4 (0.0 ppm). ^{11}B NMR chemical shifts are reported with respect to external $BF_3 \cdot OEt_2$ (δ 0.0 ppm). Magnetic moments were obtained by the method of Evans.[37] UV−visible spectra were recorded on a Cary 5000 UV−vis−NIR spectrophotometer. For the variable-temperature UV−vis experiment, the sample in the cuvette was cooled and heated by an external cooler regulated by the Peltier effect. Magnetization measurements were performed on a Quantum Design SQuID susceptometer at 0−5 Tesla and 2−300 K. Susceptibility data were fitted using the program JulX, version 1.3, written by Dr. Eckhard Bill, Max-Planck-Institut für Bioanorganische Chemie, Mühlheim an der Ruhr, Germany. X-ray diffraction data were collected on a SMART6000 (Bruker) system under a stream of N_2 (g) at low temperatures. The EPR measurements were performed in quartz tubes equipped with J-young valves. EPR data for **4** were recorded with a Bruker EMX EPR instrument. Other EPR spectra were recorded on a JEOL continuous wave spectrometer JES-FA200 equipped with an X-band Gunn diode oscillator, a cylindrical mode cavity, and a helium cryostat. EPR data were simulated using the full matrix diagonalization program ESRSIM written by Høgni Weihe, University of Copenhagen, Denmark.[38]

Table 2. Molecular Weight (MW) Determinations from Melting Point Determination of Four Samples of **2** in Naphthalene (napth)[a]

	T	ΔT	MW
napth (average)	80.25		
sample 1	80.08	0.17	259
sample 2	80.12	0.13	339
sample 3	80.13	0.12	367
sample 4	80.17	0.08	551

[a] Temperatures are reported in °C. The rate of heating was 0.005 °C/sec.

Molecular Weight Determination. This procedure follows an earlier protocol reported by Holland and co-workers.[24] A mixture of **2** (1.8 mg) and naphthalene (sublimed, 185 mg) was heated until an brown solution formed. After cooling, an aliquot of the brown solid was placed in a capillary, which was then plugged with silicone grease and flame-sealed. Melting point depressions, compared to that of authentic naphthalene (average of two sample runs which were sublimed prior to usage), were measured on a Thomas-Hoover melting point apparatus, using a VWR Precision 0.01 Thermometer equipped with a Pt-100Ω sensor. Molecular weights were determined using the formula molecular weight = $K \cdot w \cdot 1000/\Delta T \cdot W$, where $K = 4.9$ for naphthalene, w = mass of complex **2**, W = mass of naphthalene, and ΔT = temperature depression. The results of these measurements (four samples) are listed in Table 2.

Cyclic Voltammetry (CV) Details. In a typical CV experiment, 0.3 M $[N(^nBu)_4]PF_6$ in THF was used as a supporting electrolyte where 15−20 mg of crystalline **1** was dissolved in ∼5 mL of TBAH solution in THF at 25 °C. A platinum disk (2.0 mm diameter, Bioanalytical Systems), a platinum wire, and a silver wire were employed as the working electrode, the auxiliary, and the reference electrode, respectively. A one-compartment cell was used in the CV measurement. The electrochemical response was collected with the assistance of an E2 Epsilon (BAS) autolab potentiostat/galvanostat with the BAS software. All of the potentials were reported against the ferrocenium/ferrocene ($Fc^{+/0}$) couple (0.0 V) measured as an internal standard, and spectra were recorded under a N_2 atmosphere.

Synthesis of Complex (PNP)NiCl (1). Complex **1** was prepared by a procedure modified from the literature, and the identity of the product was confirmed by ^1H and ^{31}P NMR spectra from independently prepared samples.[4] In a 500 mL round-bottom flask, $NiCl_2(THF)_{1.5}$ (500 mg, 2.10 mmol) was suspended in toluene (250 mL), and Li(PNP) (915.50 mg, 2.10 mmol) in 10 mL of toluene was added dropwise to the suspension. The mixture was stirred for 12 h at room temperature, after which the volatiles were evaporated completely in vacuo. The residue was extracted with toluene and filtered and the filtrate concentrated and cooled to −35 °C to afford green crystals of (PNP)NiCl (**1**) (1.05 g, 2.02 mmol,

(31) Halpern, J. *Pure Appl. Chem.* **1979**, *51*, 2171.
(32) Pangborn, A. B.; Giardello, M. A.; Grubbs, R. H.; Rosen, R. K.; Timmers, F. J. *Organometallics* **1996**, *15*, 1518.
(33) Eckert, N. A.; Bones, E. M.; Lachicotte, R. J.; Holland, P. L. *Inorg. Chem.* **2003**, *42*, 1720.
(34) Schwindt, M. A.; Lejon, T.; Hegedus, L. S. *Organometallics* **1990**, *9*, 2814.
(35) Miller, J. B. *J. Org. Chem.* **1959**, *24*, 560.
(36) Dias, H. V. R.; Power, P. P. *J. Am. Chem. Soc.* **1989**, *111*, 144.
(37) (a) Sur, S. K. *J. Magn. Reson.* **1989**, *82*, 169. (b) Evans, D. F. *J. Chem. Soc.* **1959**, 2003.
(38) Jacobsen, C. J. H.; Pedersen, E.; Villadsen, J.; Weihe, H. *Inorg. Chem.* **1993**, *32*, 1216.

96% yield). Anal. calcd for $C_{26}H_{40}NP_2NiCl$: C, 59.74; H, 7.71; N, 2.68. Found: C, 60.92; H, 7.69; N, 2.46. Mp: 178(2) °C.

Synthesis of Complex [Ni(μ_2-PNP)]$_2$ (2). Compound **1** (200 mg, 0.38 mmol) was taken in a vial with ∼5 mL of THF and the solution cooled to −35 °C. An analogously cold suspension of KC_8 in THF (56 mg, 0.42 mmol) was added to the nickel solution. The reaction mixture was stirred for 1 h, and the dark suspension was then dried under reduced pressure. The dried mass was extracted with hexane and filtered and the filtrate kept cold (−35 °C) for two days to isolate brown crystals of [Ni(μ_2-PNP)]$_2$ (**2**) (115 mg, 0.12 mmol, 62% yield). ^{1}H NMR (25 °C, 399.8 MHz, C_6D_6): δ 16.68 (br, $\nu_{1/2}$ = 279 Hz), 8.41 (br, $\nu_{1/2}$ = 96 Hz), 4.53 (br, $\nu_{1/2}$ = 53 Hz), 2.85 (br, $\nu_{1/2}$ = 347 Hz), 1.25 (br, $\nu_{1/2}$ = 22 Hz), 0.89 (br, $\nu_{1/2}$ = 6 Hz). μ_{eff}: 2.84 (1) μ_B (C_6D_6, 25 °C, Evans method). Anal. calcd for $C_{52}H_{80}N_2P_4Ni$: C, 64.08; H, 8.23; N, 2.87. Found: C, 64.36; H, 8.17; N, 2.86. UV−vis (hexane, λ in nm, ε in mol^{-1} cm^{-1}): 616 (826), shoulder at 475 (2521), shoulder at 438 (4526), shoulder at 390 (8383). Mp: 148(2) °C.

Bond Splitting Reaction of 2 with H_2. Synthesis of Complex (PNP)NiH (3). In a J-Young tube, complex **2** (40 mg, 0.041 mmol) was dissolved in C_6D_6 and degassed by a standard freeze−pump−thaw technique. An excess amount of dihydrogen gas was passed through the solution, during which the brown color changed to yellowish after 10 min. Examination by ^{1}H and ^{31}P NMR spectra confirmed the quantitative formation of compound **3**.

Synthesis of Complex Ni(PNP=NNCPh$_2$) (4). In a vial, **2** (75 mg, 0.08 mmol) was dissolved in ∼5 mL of hexane and cooled to −35 °C. In a separate vial, Ph_2CN_2 (29.9 mg, 0.15 mmol) was taken in hexane and cooled to −35 °C. Ph_2CN_2 solution was added dropwise to **2** and stirred for 2 h. During the course of the reaction (∼20 min), a brown-colored precipitate appeared. After completion of the reaction, the reaction mixture was filtered, and the brown-colored residue was collected and washed with 10 mL of hexane. The product was dried and redissolved in a minimum of toluene (∼2 mL), and then two drops of hexane in a toluene solution were added, from which brown-colored crystals were obtained at −35 °C (63.8 mg, 0.09 mmol, 61% yield). ^{1}H NMR (25 °C, 399.8 MHz, C_6D_6): δ 8.21 (br, $\nu_{1/2}$ = 36 Hz), 7.69 (m, aryl), 7.35 (m, aryl), 7.02 (m, aryl), 2.11−1.99 (br, *Me*Ar and C*H*Me$_2$ resonances overlapped), 1.23 (br, CH*Me*$_2$), 0.89 (br, CH*Me*$_2$). μ_{eff}: 2.22(3) μ_B (C_6D_6, 25 °C, Evans method). Mp: 118(2) °C. Multiple attempts to obtain satisfactory combustion analysis data failed given the thermal instability of the complex.

Bond-Splitting Reaction of 2 with H_2O. Synthesis of Complex (PNP)Ni(OH) (5) and 3. In a Schlenk flask, complex **2** was dissolved (60 mg, 0.062 mmol) in 20 mL of THF. To the solution was added degassed water (purged with argon over 10 min, 0.04 mL, 1.24 mmol) by means of cannula transfer. The solution was stirred for 2 h, during which the color of the reaction mixture rapidly changed from brown to green. After the completion of the reaction, the solution was dried under reduced pressure. ^{1}H and ^{31}P NMR spectra of the reaction mixture revealed an equimolar formation of **3** and **5**.

Bond-Splitting Reaction of 2 with CH_3OH. Synthesis of Complex (PNP)Ni(OCH$_3$) (6) and 3. CH_3OH (10 mL) was stirred over a few pieces of thin sodium film (∼500 mg) for 16 h and the solution filtered through alumina to obtain the anhydrous reagent. Complex **2** (60 mg, 0.062 mmol) was taken in a vial and dissolved in THF (5 mL). To the brown solution was added via syringe anhydrous CH_3OH (1.98 mg, 0.062 mol) and the mixture stirred. Over the course of 2 h, the reaction mixture gradually changed from brown to reddish brown. After 2 h of stirring, the reaction mixture was dried in vacuo. ^{1}H and ^{31}P NMR spectra confirmed the formation of **3** and **6** in an equimolar amount.

Bond-Splitting Reaction of 2 with H_2PPh. Synthesis of Complex (PNP)Ni(PHPh) (7) and 3. In a vial was dissolved **2** (40 mg, 0.041 mmol) in 5 mL of THF and the solution cooled to −35 °C. An analogously cooled solution of phenylphosphine (4.52 mg, 0.041 mmol) in 2 mL of hexane was added dropwise to the cooled solution of **2**. The reaction mixture was stirred for 2 h, during which the color of the solution changed immediately from brown to red. The solution was then dried under reduced pressure, and ^{1}H and ^{31}P NMR spectra confirmed an equimolar formation of compounds **3** and **7**.

Bond-Splitting Reaction of 2 with HB(catechol). Synthesis of Complex (PNP)Ni[B(catechol)]) (8) and 3. In a vial, compound **2** (50 mg, 0.053 mmol) was dissolved in 5 mL of hexane and the solution cooled to −35 °C. In a separate vial, an analogously cooled solution of catecholborane (6.28 mg, 0.053 mmol) in hexane was added dropwise to the Ni(I) solution. The solution was stirred for 3 h, during which the color gradually changed from brown to yellowish. The solution was evaporated to dryness, and ^{1}H and ^{31}P NMR spectra of the mixture confirmed an equimolar formation of **8** and **3** as the only two products.

Attempted Bond Splitting Reaction of 2 with NH_3. Complex **2** (60 mg, 0.062 mol) was taken in a Schlenk flask in ∼5 mL of THF and in situ generated NH_3 [generated from $LiNH_2$ (7.02 mg, 0.31 mmol) and 2,6-diisopropylphenol (22.05 mg, 0.31 mmol) in ∼ 10 mL THF] was passed through a vacuum adapter. The solution was stirred for 1 h, during the course of which the color of the nickel solution changed from brown to green. ^{1}H and ^{31}P NMR spectra of the reaction revealed the formation of equimolar amounts of **3** and **5**. Attempts to generate dry NH_3 from Na/NH_3 electride solution also resulted in the quantitative formation of **3** and **5** from **2**.

Synthesis of Complex (PNP)Ni(NH$_2$) (9). Complex **1** (150 mg, 0.29 mmol) was dissolved in diethyl ether (∼5 mL) and cooled to −35 °C, and a suspended solution of $NaNH_2$ (11.5 mg, 0.29 mmol) in diethyl ether was added dropwise. After stirring the reaction mixture for 8 h, the mixture was filtered and concentrated to ∼2 mL. The concentrated solution was cooled to −35 °C for 48 h to yield green crystals of **9** (99 mg, 0.20 mmol, 69% yield). ^{1}H NMR (25 °C, 399.8 MHz, C_6D_6): δ 7.58 (d, 2H, C_6H_3), 6.97 (s, 2H, C_6H_3), 6.77 (d, 2H, C_6H_3), 2.16−2.02 (br, 4H, C*H*Me$_2$), 2.12 (s, 6H, *Me*Ar), 1.40 (dd, 12H, CH*Me*$_2$), 1.26 (dd, 12H, CH*Me*$_2$), −2.30 (t, 2H, N*H*$_2$). ^{13}C NMR (25 °C, 100.6 MHz, C_6D_6): δ 162.05 (aryl), 132.06 (aryl), 131.86 (aryl), 123.87 (aryl), 120.64 (aryl), 116.07 (aryl), 23.86 (*C*HMe$_2$), 20.56 (M*e*Ar), 18.74 (CH*Me*$_2$), 17.99 (CH*Me*$_2$). ^{31}P NMR (25 °C, 121.5 MHz, C_6D_6): δ 30.77. MS-CI, [M + H]$^+$: calcd, 502.217; found, 502. 189. Mp: 166(3) °C.

Independent Synthesis of Complex 5. Method A. Complex **1** (120 mg, 0.24 mmol) was dissolved in 50 mL of THF in a Schlenk flask. In a separate Schlenk flask, KOH (752 mmol solution, large excess) in water (1.92 mL, 1.44 mmol) was deareated by a standard freeze−pump−thaw technique. To the cold (−78 °C) solution of nickel, the KOH solution in water was transferred via cannula, and the reaction mixture was slowly allowed to warm up to room temperature. After 4 h of stirring, the reaction mixture was dried under reduced pressure and extracted with pentane. The green-colored extract was filtered and cooled to isolate the desired product, **5** (53.2 mg, 0.106 mmol, 46% yield). The low yield was due to the unachieved completion of the reaction, supposedly stemming from the solubility of byproduct KCl, which can drive the reaction in the backward direction. Crude product was always isolated along with the contamination of **1**. **Method B.** In a Schlenk flask, complex **9** (100 mg, 0.20 mmol) was dissolved in 10 mL of hexane. An

excess amount of deoxygenated water was added dropwise under a positive pressure of N_2 and the solution stirred for 10 min. After this time, the solution was dried in vacuo, and a green-colored product was collected (96 mg, 0.19 mmol, 96% yield). ^{1}H NMR (25 °C, 399.8 MHz, C_6D_6): δ 7.52 (d, 2H, C_6H_3), 6.92 (s, 2H, C_6H_3), 6.70 (d, 2H, C_6H_3), 2.28−2.10 (br, C*H*Me$_2$, 4H), 2.16 (s, 6H, *Me*Ar), 1.51 (dd, 12H, CH*Me*$_2$), 1.29 (dd, 12H, CH*Me*$_2$), −5.06 (t, 1H, O*H*). ^{13}C NMR (25 °C, 100.6 MHz, C_6D_6): δ 162.26 (aryl), 132.10 (aryl), 131.94 (aryl), 124.16 (aryl), 120.78 (aryl), 116.94 (aryl), 23.46 (*C*HMe$_2$), 20.49 (*Me*Ar), 18.62 (CH*Me*$_2$), 17.87 (CH*Me*$_2$). ^{31}P NMR (25 °C, 121.5 MHz, C_6D_6): δ 26.89. MS-CI $[M + H]^+$: calcd, 502.217; found, 502. 189 along with 486.2 corresponding to (PNP)Ni$^+$. Mp: 82(2) °C.

Independent Synthesis of Complex 6. In a Schlenk flask, complex **1** (300 mg, 0.60 mmol) was dissolved in 50 mL of THF. In a separate Schlenk flask, **1** was charged with KOH in methanol (0.58 mL, 0.60 mmol) and deaerated by a standard freeze−pump−thaw technique. To the cold solution (−78 °C) of nickel, the KOH in methanol was transferred via cannula, and the reaction mixture was allowed to warm up to room temperature. After 3 h of stirring, the reaction mixture was dried in vacuo, extracted with pentane, and filtered. From the filtrate, brown-colored crystals of (PNP)Ni(OCH$_3$) (**6**) were isolated after cooling the solution to −35 °C for 48 h (234 mg, 0.45 mmol, 79% yield). ^{1}H NMR (25 °C, 399.8 MHz, C_6D_6): δ 7.43 (d, 2H, C_6H_3), 6.92 (s, 2H, C_6H_3), 6.71(d, 2H, C_6H_3), 3.30 (s, 3H, OCH_3), 2.28−2.12 (br, 4H, C*H*Me$_2$), 2.15 (s, 6H, *Me*Ar), 1.54 (dd, 12H, CH*Me*$_2$), 1.32 (dd, 12H, CH*Me*$_2$). ^{13}C NMR (25 °C, 100.6 MHz, C_6D_6): δ 162.26 (aryl), 132.12 (aryl), 131.95 (aryl), 124.52 (aryl), 120.03 (aryl), 116.61 (aryl), 57.37 (O*C*H$_3$), 23.63 (*C*HMe$_2$), 20.50 (*Me*Ar), 18.52 (CH*Me*$_2$), 17.78 (CH*Me*$_2$). ^{31}P NMR (25 °C, 121.5 MHz, C_6D_6): δ 24.61. MS-CI $[M + H]^+$: calcd, 517.217; found, 517.215. Mp: 128(2) °C.

Independent Synthesis of Complex 7. Complex **1** (100 mg, 0.19 mmol) was dissolved in 10 mL of diethyl ether and cooled to −35 °C. In a separate vial, LiPHPh (22.2 mg, 0.19 mmol) was dissolved and the solution cooled to −35 °C. A LiPHPh solution was added dropwise to the nickel solution, and the color changed to reddish brown after 5 min. After allowing the mixture to stir for 2 h, the volatiles were removed under reduced pressure, the solid extracted with pentane, and the solution filtered. The filtrate was then concentrated and cooled to −35 °C over 4 days to afford red crystals of (PNP)Ni(PHPh) (**7**) (81 mg, 0.14 mmol, 71% yield). ^{1}H NMR (25 °C, 399.8 MHz, C_6D_6): δ 8.01 (t, 1H, PHAr), 7.68 (d, C_6H_3, 2H), 7.09−6.98 (br, 4H, C_6H_3), 6.94 (d, 2H, PHAr), 6.84 (d, 2H, PHAr), 3.64 (doublet of triplets, 1H, NiP*H*Ph), 2.23−2.11 (br, 4H, C*H*Me$_2$), 2.18 (s, 6H, *Me*Ar), 1.26 (dd, 12H, CH*Me*$_2$), 1.11 (dd, 12H, CH*Me*$_2$). ^{13}C NMR (25 °C, 100.6 MHz, C_6D_6): δ161.24 (aryl), 136.67 (aryl), 132.44 (aryl), 132.04 (aryl), 129.33 (aryl), 127.50 (aryl), 126.00 (aryl), 124.33 (aryl), 121.02 (aryl), 115.53 (aryl), 24.70 (*C*HMe$_2$), 20.64 (*Me*Ar), 19.02 (CH*Me*$_2$), 17.83 (CH*Me*$_2$). ^{31}P NMR (25 °C, 121.5 MHz, C_6D_6): δ −59.33 (Ar*P*^{i}Pr$_2$, $^3J_{P-H}$ = 20 Hz), 38.36 (*P*HAr, $^1J_{P-H}$ = 179 Hz). Anal. calcd for $C_{32}H_{46}NP_3Ni$: C, 64.45; H, 7.77; N, 2.35. Found: C, 64.59; H, 7.92; N, 2.39. Mp: 72(2) °C.

Independent Synthesis of Complex 8. In a vial, complex **2** (100 mg, 0.10 mmol) was taken in hexane and the solution cooled to −35 °C. An analogously cooled solution of dicatechol diborane, (catechol)$_2$B$_2$ (16.9 mg, 0.10 mmol), was added dropwise to the Ni(I) solution. During the course of the reaction, the solution color slowly changed from brown to yellow. After 3 h of stirring, the solution was dried in vacuo, the solid extracted with ether and filtered, and the filtrate concentrated. The ether solution was kept at −35 °C for 24 h, from which yellow-colored crystals of **8** were obtained (55 mg, 0.09 mmol, 45% yield). ^{1}H, ^{31}P, and ^{11}B NMR spectroscopic data confirmed the formation of **8** when compared to those of an independently prepared sample.[25]

Synthesis of Complex (PNP)Ni(SPh) (10). Complex **2** (20 mg, 0.021 mmol) and diphenyldisulfide (4.6 mg, 0.021 mmol) were loaded into a J-Young tube in hexane. No immediate color change was observed after the loading. The reaction mixture was stirred for an hour, and the brown color of the solution was intensified during the course of the reaction. The mixture was monitored by ^{31}P NMR spectroscopy until complete (1 h). After this time, the reaction mixture was dried in vacuo, and the ^{1}H NMR spectrum showed quantitative formation of the product, **10**. ^{1}H NMR (25 °C, 399.8 MHz, C_6D_6): δ 8.04 (d, SC$_6H_5$, 2H), 7.54 (d, C_6H_3, 2H), 7.02 (t, SC$_6H_5$, 1H), 6.89 (m, overlapped resonances of aryl protons, 4H), 6.77 (d, C_6H_3, 2H), 2.22−2.08 (br, C*H*Me$_2$, 4H), 2.14 (s, *Me*Ar, 6H), 1.40 (dd, CH*Me*$_2$, 12H), 1.17 (dd, CH*Me*$_2$, 12H). ^{13}C NMR (25 °C, 100.6 MHz, C_6D_6): δ 162.04 (aryl), 133.33 (aryl), 132.47 (aryl), 131.81 (aryl), 129.33 (aryl), 127.66 (aryl), 125.02 (aryl), 122.02 (aryl), 121.41 (aryl), 116.15 (aryl), 24.54 (*C*HMe$_2$), 20.53 (*Me*Ar), 18.53 (CH*Me*$_2$), 17.65 (CH*Me*$_2$). ^{31}P NMR (25 °C, 121.5 MHz, C_6D_6): 33.65 ppm. NMR spectra (^{1}H, ^{31}P, and ^{13}C) are included in the Supporting Information as proof of bulk purity.

Synthesis of Complex (PNP)Ni(SePh) (11). Complex **2** (20 mg, 0.021 mmol) and diphenyldiselenide (6.6 mg, 0.021 mmol) were loaded into a J-Young tube along with hexane. The reaction mixture was stirred for an hour and monitored by ^{31}P NMR spectroscopy, and during the course of the reaction, the brown color of the solution was intensified. After 1 h, the reaction mixture was dried in vacuo, and the ^{1}H NMR spectrum showed quantitative formation of the product, **11**. ^{1}H NMR (25 °C, 399.8 MHz, C_6D_6): δ 8.07 (d, SC$_6H_5$, 1H), 7.54 (m, overlapped resonances of aryl protons, 2H), 6.95 (m, overlapped resonances of aryl protons, 6H), 6.79 (d, C_6H_3, 2H), 2.21−2.06 (br, C*H*Me$_2$, 4H), 2.15 (s, *Me*Ar, 6H), 1.41 (dd, CH*Me*$_2$, 12H), 1.18 (dd, CH*Me*$_2$, 12H). ^{13}C NMR (25 °C, 100.6 MHz, C_6D_6): δ 161.70 (aryl), 136.28 (aryl), 132.39 (aryl), 131.90 (aryl), 131.73 (aryl), 129.40 (aryl), 124.94 (aryl), 124.00 (aryl), 121.86 (aryl), 116.13 (aryl), 24.83 (*C*HMe$_2$), 20.54 (*Me*Ar), 18.94 (CH*Me*$_2$), 17.84 (CH*Me*$_2$). ^{31}P NMR (25 °C, 121.5 MHz, C_6D_6): 36.44 ppm. NMR spectra (^{1}H, ^{31}P, and ^{13}C) are included in the Supporting Information as proof of bulk purity.

Crystallographic Details. Single crystals of **2**·Et$_2$O (Et$_2$O), **4**·Et$_2$O (Et$_2$O), **5** (pentane), and **9** (Et$_2$O) were grown at −35 °C from concentrated solutions. Inert-atmosphere techniques were used to place the crystal onto the tip of a diameter glass capillary (0.05 mm) mounted on a SMART6000 (Bruker) at 113−137(2) K. A preliminary set of cell constants was calculated from reflections obtained from three nearly orthogonal sets of 10−30 frames. The data collection was carried out using graphite-monochromated Mo Kα radiation with a frame time of 10 s and a detector distance of 5.0 cm. A randomly oriented region of a sphere in reciprocal space was surveyed. In general, three sections of 606 frames were collected with 0.30° steps in ω at different ϕ settings with the detector set at −43° in 2θ. Final cell constants were calculated from the *xyz* centroids of strong reflections from the actual data collection after integration (SAINT).[39] The structure was solved using SHELXS-97 and refined with SHELXL-97.[40]

Crystallographic Details for 2·Et$_2$O. The crystals occurred as very small dark needles that appeared to have a red or green tinge. Several crystals were examined and were found to be twinned, and

(39) *SAINT*, 6.1 ed.; Bruker Analytical X-ray Systems: Madison, WI, 1991−2003.
(40) *SHELXL-Plus*, 5.10 ed.; Bruker Analytical X-ray Systems: Madison, WI, 1999.

the structure was initially solved using a twinned crystal. Further examination revealed a single crystal of approximate dimensions 0.20 × 0.05 × 0.04 mm, which was used as the sample. Intensity statistics and systematic absences suggested the centrosymmetric space group $P2_1/c$, and subsequent solution and refinement confirmed this choice. A direct-methods solution was calculated which provided most non-hydrogen atoms from the E-map. Full-matrix least-squares/difference Fourier cycles were performed, which located the remaining non-hydrogen atoms. A slight disorder occurs in one isopropyl group, and a diethyl ether solvent is present. All non-hydrogen atoms were refined with anisotropic displacement parameters. With the exception of those associated with the disordered atoms, all hydrogen atoms were located in subsequent Fourier maps and included as isotropic contributors in the final cycles of refinement. All hydrogen atoms associated with the disorder were placed in ideal positions and refined as riding atoms with relative isotropic displacement parameters.

Crystallographic Details for 4·Et$_2$O. The sample consisted of extremely small red needles of maximum diameter of only a few microns. Inert atmosphere techniques were used to place a typical crystal of dimensions 0.20 × 0.03 × 0.03 mm onto the tip of a 0.02-mm-diameter glass fiber. Intensity statistics and systematic absences suggested the centrosymmetric space group $P2_1/c$, and subsequent solution and refinement confirmed this choice. A direct-methods solution was calculated, which provided most non-hydrogen atoms from the E-map. Full-matrix least-squares/difference Fourier cycles were performed, which located the remaining non-hydrogen atoms. Non-hydrogen atoms were refined with anisotropic displacement parameters except for two carbon atoms that converged to nonpositive values. The latter were refined isotropically. All hydrogen atoms were placed in ideal positions and refined as riding atoms with relative isotropic displacement parameters.

Crystallographic Details for 5. Crystals were typically elongated parallelogram-shaped prisms of varying sizes. Inert atmosphere techniques were used to place a typical crystal of approximate dimensions 0.30 × 0.13 × 0.05 mm. Intensity statistics and systematic absences suggested the centrosymmetric space group $P2_1/n$, and subsequent solution and refinement confirmed this choice. A direct-methods solution was calculated, which provided most non-hydrogen atoms from the E-map. Full-matrix least-squares/difference Fourier cycles were performed, which located the remaining non-hydrogen atoms. All non-hydrogen atoms were refined with anisotropic displacement parameters. After the conclusion of the initial refinement, it was recognized that there was a "ghost" image of the molecule translated by 0.5 along the *a* axis. Using the SAME command in SHELX, it was possible to refine to a suitable model with a relative occupancy of 0.958:0.042. Examination of the packing reveals that the molecules are stacked in channels parallel to the *a* axis. Two additional crystals were examined, and the same translational disorder was located, differing only in the occupancy. All hydrogen atoms were placed in ideal positions and refined as riding atoms with relative isotropic displacement parameters.

Crystallographic Details for 9. Inert atmosphere techniques were used to place a green crystal of approximate dimensions 0.15 × 0.10 × 0.03 mm. Several other crystals were examined, and all were badly split or twinned. During data collection, two major components were identified using George Sheldrick's CELL_NOW program. The Bruker-AXS SAINT program was used to generate an HKL5 file that was used in the refinement. The intensity data were corrected for absorption (TWINABS).[41] Intensity statistics and systematic absences suggested the centrosymmetric space group $P\bar{1}$, and subsequent solution and refinement confirmed this choice. A direct-methods solution was calculated, which provided most non-hydrogen atoms from the E-map. Full-matrix least-squares/difference Fourier cycles were performed, which located the remaining non-hydrogen atoms. It was necessary to use isotropic thermal parameters for several of the atoms, and examination of the ORTEP drawings shows that the model is not 100% agreeable. All hydrogen atoms were placed in ideal positions and refined as riding atoms with relative isotropic displacement parameters. It was not possible to locate the two hydrogens on the N atom.

Acknowledgment. We thank Indiana University—Bloomington, the Dreyfus Foundation, the Sloan Foundation, the NSF (CHE-0348941, PECASE award to D.J.M.), and the Chemical Sciences, Geosciences and Biosciences Division, Office of Basic Energy Science, Office of Science, U.S. Department of Energy (DE-FG02-07ER15893) for financial support of this research. Mr. Patrick Feng is also acknowledged for collecting preliminary magnetization data for **2**. Professor Patrick L. Holland is acknowledged for his assistance in molecular weight determination by the freezing point depression method. K.M. acknowledges the DFG (SFB583) for financial support. Dr. Maren Pink is also thanked for insightful comments to the crystallographic studies presented in this work.

Supporting Information Available: Complete crystallographic data (**2**, **4**, **5**, and **9**), figures, and additional discussion. This material is available free of charge via the Internet at http://pubs.acs.org.

IC801137P

(41) An empirical correction for absorption anisotropy was used: Blessing, R. *Acta Crystallogr.* **1995**, *A51*, 33.